Inorg. Chem. **2003**, *42*, 7249–7257

Kinetic Stability of the Peroxidase Activity of Unfolded Cytochrome *c*: Heme Degradation and Catalyst Inactivation by Hydrogen Peroxide

Rutger E. M. Diederix,[†] Maria Fittipaldi,[‡] Jonathan A. R. Worrall,[†] Martina Huber,[‡] Marcellus Ubbink,*[,†] and Gerard W. Canters[†]

Gorlaeus Laboratories, Leiden Institute of Chemistry, Leiden University, P.O. Box 9502, 2300 RA Leiden, The Netherlands, and Department of Molecular Physics, Leiden University, P.O. Box 9504, 2300 RA Leiden, The Netherlands

Received April 11, 2003

Unfolding converts *Paracoccus versutus* cytochrome *c*-550 into a potent peroxidase (Diederix, R. E. M.; Ubbink, M.; Canters, G. W. *ChemBioChem* **2002**, *3,* 110–112). The catalytic activity is accompanied by peroxide-driven inactivation that is prevented, in part, by reducing substrate. Here, the kinetics of inactivation are described, and evidence is presented for the occurrence of a labile intermediate on the catalytic peroxidase pathway of unfolded cytochrome *c*-550. This intermediate represents a branching point, whereby the protein proceeds along either the productive pathway or self-inactivates. Reducing substrate suppresses inactivation by decreasing the steady-state concentration of the labile intermediate. Inactivation is accompanied by heme degradation. Its chemical reactivity, UV–vis, and EPR properties identify the first intermediate as hydroxyheme-cytochrome *c*-550, i.e. with heme hydroxylated at one of the heme meso positions. The occurrence of this species argues for the peroxo-iron species in the peroxidase mechanism as the labile intermediate leading to inactivated cytochrome *c*-550.

Peroxidases are heme containing enzymes, capable of catalyzing a wide array of reactions, including oxidative dehydrogenation, oxygen transfer, and peroxidative halogenations.[1,2] The potential use of these enzymes is considerable, especially since they utilize the environmentally benign oxidant H_2O_2 to perform these oxidation reactions. Relevant applications of peroxidases are in pulp bleaching, in the degradation of aromatics and halogenated xenobiotics, and in the synthesis of fine chemicals. To date, heme peroxidases are applied as components of biosensors and in immunoassays.[2] However, the usefulness of peroxidases in these reactions is limited by their poor stability in the presence of H_2O_2, which rapidly inactivates these enzymes.[1,2] Other heme-containing proteins, such as hemo- and myoglobins, and cytochrome *c* can also catalyze peroxidation reactions, but at much lower reaction rates.[3−7] These proteins are promising candidates for the mentioned applications, but unfortunately, they are also prone to H_2O_2-driven inactivation and heme degradation.[2,3,5,7] Understanding the mechanism of inactivation may help to improve the applicability of these proteins.

For this reason, we set out to study the inactivation mechanism and heme degradation pathway in Gdn·HCl-unfolded cytochrome *c*-550 (u-cytc550) from *Paracoccus versutus* (cytc550). The peroxidase activity of both native and u-cytc550 has been characterized.[7−9] In its native form, this electron-transport protein contains hexacoordinate heme-iron and has low peroxidase activity.[7] Unfolding causes release of the native heme methionine ligand, which results in a significant increase in the peroxidase reaction rate.[8,9] U-cytc550 is thus a much more useful catalyst than native cytc550, which is why we have chosen it for this study.

* To whom correspondence should be addressed. E-mail: m.ubbink@chem.leidenuniv.nl. Phone: +31 71 527 4628. Fax: +31 71 527 4593.
[†] Gorlaeus Laboratories, Leiden Institute of Chemistry.
[‡] Department of Molecular Physics.

(1) van Deurzen, M. P. J.; van Rantwijk, F.; Sheldon, R. A. *Tetrahedron* **1997**, *53*, 13183−13220.
(2) Valderrama, B.; Ayala, M.; Vazquez-Duhalt, R. *Chem. Biol.* **2002**, *9*, 555−565.
(3) Raven, E. L.; Mauk, A. G. *Adv. Inorg. Chem.* **2001**, *51*, 1−49.
(4) Everse, J.; Johnson, M. C.; Marini, M. A. *Methods Enzymol.* **1994**, *231*, 547−561.
(5) Vazquez-Duhalt, R. *J. Mol. Catal. B*: *Enzym.* **1999**, *7*, 241−249.
(6) Ozaki, S.-I.; Matsui, S.; Roach, M. P.; Watanabe, Y. *Coord. Chem. Rev.* **2000**, *198*, 39−59.
(7) Diederix, R. E. M.; Ubbink, M.; Canters, G. W. *Eur. J. Biochem.* **2001**, *268*, 4207−4216.
(8) Diederix, R. E. M.; Ubbink, M.; Canters, G. W. *ChemBioChem* **2002**, *3*, 110−112.
(9) Diederix, R. E. M.; Ubbink, M.; Canters, G. W. *Biochemistry* **2002**, *41*, 13067−13077.

10.1021/ic0343861 CCC: $25.00
Published on Web 10/04/2003

Moreover, the faster reaction rates of u-cytc550 facilitate the study of the heme degradation pathway, which in native cytc550 is obscured because of the very slow first step in the reaction of the protein with H_2O_2.[7]

Herein, the peroxide-driven inactivation mechanism and heme degradation pathway of u-cytc550 are described. The kinetics of inactivation demonstrate the presence of a labile intermediate in the peroxidase cycle of u-cytc550, with an inherent tendency for self-inactivation. Transient kinetics studies indicate the occurrence of at least three species in the heme degradation pathway. The first degradation intermediate could be isolated in a stable form, and characterization by UV−vis and EPR spectroscopy identified it as hydroxyheme-containing cytc550. This makes it likely that the labile intermediate in the peroxidase cycle of u-cytc550 is the peroxo-iron species.

Experimental Section

P. versutus cytc-550 was produced in *P. denitrificans* strain 2131 and isolated as described.[7] Chemicals were of the highest grade commercially available and dissolved in deionized water (Milli-Q). Gdn·HCl (Biochemika grade, Fluka) was dissolved to 8 M, and this stock solution was filtered over 0.45 μM HV Durapore filters (Millipore) before use. The solutions were buffered with 0.1 M sodium phosphate, and all experiments were performed in 6 M Gdn·HCl. Unless stated otherwise, the pH of each solution was 5.0, measured separately with a Corning pH pencil gel combo-electrode calibrated with IUPAC standard buffers (Radiometer Analytical, France). All experiments were performed at 298 K.

The inactivation kinetics and catalytic efficiency of u-cytc550 were studied using the peroxidase assay with *o*-methoxyphenol (guaiacol, (gc)) as the reducing substrate, as described before.[7] Formation of product was followed using a Shimadzu UVPC-2101PC spectrophotometer fitted with a thermostat. It was assumed that the product of the reaction, tetraguaiacol ($\epsilon_{470} = 26.6$ mM^{-1} cm^{-1}) was the result of four oxidation reactions.[10] The inactivation rate was determined by fitting the product formation curves to a first-order process for catalyst inactivation. The catalytic efficiency (i.e., the amount of gc turnovers before catalyst inactivation) was determined by subtracting the initial absorption from the final absorption at 470 nm (after full completion of the reactions) and dividing this by the concentration of u-cytc550 employed. In the inactivation rate and catalytic efficiency measurements, [u-cytc550] was varied between 0.2 and 1 μM, [H_2O_2] between 2.5 and 100 mM, and [gc] between 1 and 50 mM.

Transient kinetics studies were performed using an Applied Photophysics SX.18 stopped-flow instrument. In some cases, the diode array (320−1000 nm) accessory was used to follow spectral evolution. Analysis of the latter and deconvolution of the spectra of individual components was performed using the Global Analysis module of the Pro-K software package (Applied Photophysics, U.K.), which makes use of the singular value decomposition algorithm.[11]

Steady-state optical measurements on the heme-degradation pathway of u-cytc550 were performed with the spectrophotometer already described. Samples containing predominantly the first heme degradation intermediate were prepared by the addition of 6 successive aliquots of 0.5 molar equiv of H_2O_2 to u-cytc550 under continuous stirring, at room temperature. After the addition of each aliquot, the reaction was allowed to proceed to completion by waiting for > 10 min. EPR samples were prepared by concentrating the thus obtained sample using a Centricon device with 10 kDa cutoff membrane (Amicon). A sample of unmodified u-cytc550 was also prepared, and the approximate concentration of protein in both samples was 1 mM. Included in the samples was 30% glycerol. X-band EPR spectra were recorded with a Bruker ELEXSYS E 680 spectrometer in which a metallic cavity was used. The measurements were performed at 40 K, using an Oxford ESR 900 H cryostat. The instrumental conditions were the following: modulation frequency 100 kHz, field modulation amplitude 0.5 mT, sweep width 0.4 T, microwave frequency 9.48 GHz, and power 20 mW.

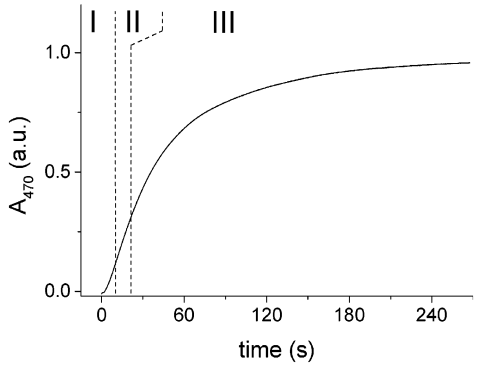

Figure 1. Typical product formation curve of u-cytc550 with H_2O_2 and gc as oxidizing and reducing substrates, respectively. Conditions: 0.4 μM cytc550, 10 mM H_2O_2, 1 mM gc, 6 M Gdn·HCl, 100 mM sodium phosphate pH 5.0, 298 K. The different phases, labeled I−III, are discussed in the text.

Results

Inactivation of the Peroxidase Activity of u-cytc550 under Turnover Conditions. A typical product formation curve due to the peroxidase activity of u-cytc550 is shown in Figure 1. The curve consists of three phases: a lag phase (I), followed by a linear phase (II), which is in turn followed by a decrease in activity ending in a plateau (III). The shape of the curve is comparable to that observed with native cytc550,[7] except that, in the presence of 6 M Gdn·HCl, no product breakdown is observed. As with native cytc550, the lag-phase is attributed to an activation process involving oxidation of protein residues.[7] When fresh u-cytc550 is added when the reaction has reached the plateau, the absorption increase starts again, and the total absorbance due to product formation after complete inactivation is linearly related to the amount of u-cytc550 initially present (not shown).

The activity decrease in time (phase III in Figure 1) could be fitted to a monoexponential function, indicating a first-order inactivation process. The rate constants are plotted in Figure 2a,b as a function of H_2O_2 and the reducing substrate, guaiacol (gc), respectively. The rate constant shows a hyperbolic dependence on [H_2O_2] (Figure 2a). In the presence of 10 mM gc, the rate constant of inactivation at saturating [H_2O_2] is 1.16 ± 0.06 s^{-1}, and the inactivation rate constant is half-maximal at 111 ± 10 mM H_2O_2. With increasing [gc], the rate constant of inactivation decreases hyperbolically (Figure 2b). The inactivation rate constant plotted against the inverse concentration of gc (Figure 2b, inset) gives a linear dependence with slope 0.25 ± 0.01 mM s^{-1} and

(10) Baldwin, D. A.; Marques, H. M.; Pratt, J. M. *J. Inorg. Biochem.* **1987**, *30*, 203−217.
(11) Henry, E. R.; Hofrichter, J. *Methods Enzymol.* **1992**, *210*, 129−192.

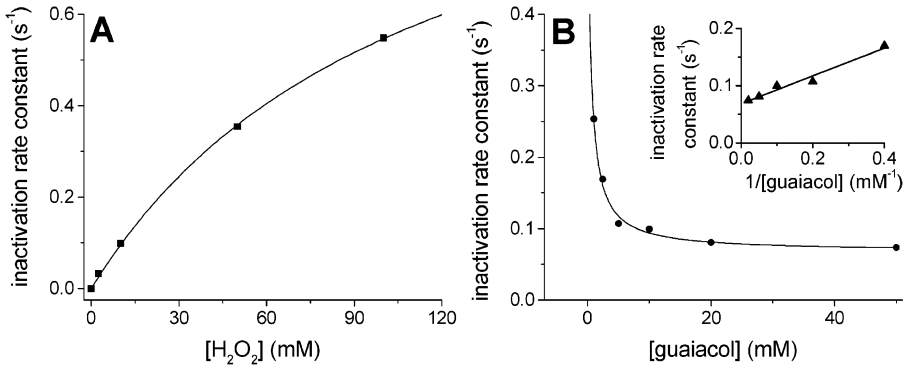

Figure 2. (a) Inactivation rate constant of u-cytc550 as a function of H_2O_2, in the presence of 10 mM gc. (b) Inactivation rate constant of u-cytc550 as a function of gc, in the presence of 10 mM H_2O_2. Inset: the inactivation rate constant plotted against the inverse [gc]. Each data point is the average of 5 different experiments, whereby [u-cytc550] was varied between 0.2 and 1.0 μM. The solid lines are best fits to the data using eq 2, as indicated in the text.

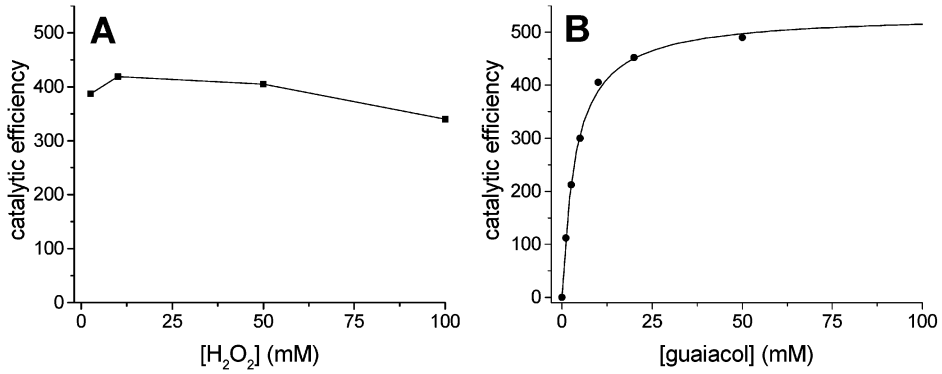

Figure 3. Catalytic efficiency (CE) of u-cytc550 as a function of H_2O_2 (a) and gc (b). In part a, [gc] was 10 mM, and in part b, [H_2O_2] was 10 mM. The CE was calculated by dividing the final concentration of product formed by [u-cytc550] initially present. Each data point is the average of 5 different experiments, whereby [u-cytc550] was varied between 0.2 and 1.0 μM.

intercept 0.067 $\pm$ 0.004 s^{-1} ([H_2O_2] = 10 mM). The latter value is the inactivation rate constant at saturating [gc]. These observations suggest the presence of an intermediate in the inactivation, formed by the reaction of u-cytc550 with H_2O_2. In turn, gc inhibits inactivation, possibly by a mechanism whereby it causes a lowering of the steady-state concentration of this intermediate.

The absorption difference (ϵ_{470} = 6650 M^{-1} cm^{-1} per oxidized gc) between the starting and end points of the product formation curves yields the amount of gc turnovers before catalyst inactivation. Divided by the amount of u-cytc550 initially present, this gives the catalytic efficiency (CE) of u-cytc550. Values of the CE thus obtained are plotted in Figure 3a,b as a function of H_2O_2 and gc, respectively. The CE of u-cytc550 is roughly constant with [H_2O_2], while it increases hyperbolically with [gc]. The maximal CE, i.e., the CE at saturating [gc] is 534 $\pm$ 10, and the CE is half-maximal at 3.7 $\pm$ 0.3 mM gc.

A potential cause for inactivation may be the adventitious generation of highly reactive species such as the hydroxyl radical, which, in principle could be formed by homolytic cleavage of the O$-$O bond of the iron-bound peroxide. This can be ruled out as a possible cause, however, because the product formation curve remained unaltered when the radical scavenger mannitol (50 mM) was included in the reaction mixture.

The Reaction of U-cytc550 with H_2O_2 in the Absence of Guaiacol. As mentioned, the inactivation of u-cytc550 may result from an intrinsic instability of a reaction product of u-cytc550 with H_2O_2. To afford insight into this, the reaction of u-cytc550 with H_2O_2 was studied in more detail, using both transient and steady-state methods. When H_2O_2 is added to u-cytc550 in the absence of gc, a number of changes take place in the UV$-$vis spectrum of u-cytc550, ultimately resulting in a severely bleached spectrum. The traces at 412.8 nm as a function of time (Figure 4a) could be fitted by a sum of three exponentials, the rate constants of which depend linearly on [H_2O_2] (Figure 4b). The fits to the data pass through the origin, and the values of the bimolecular rate constants (k_1, k_2, and k_3) are 1226 $\pm$ 7 M^{-1} s^{-1}, 309 $\pm$ 3 M^{-1} s^{-1} and 63 $\pm$ 0.6 M^{-1} s^{-1}. The rate constants were identical at 1 and 5 μM u-cytc550 (not shown). This corresponds to a reaction as in Scheme 1:

Scheme 1

$$\mathrm{A} \xrightarrow{k_1[\mathrm{H_2O_2}]} \mathrm{B} \xrightarrow{k_2[\mathrm{H_2O_2}]} \mathrm{C} \xrightarrow{k_3[\mathrm{H_2O_2}]} \mathrm{D} \qquad (1)$$

The bimolecular rate constant of the reaction of u-cytc550 with H_2O_2 was previously measured under turnover conditions, giving a value of 1500 M^{-1} s^{-1}, assuming each peroxide oxidizes two gc molecules.[8] This value is similar to the rate constant for the first phase (1226 M^{-1} s^{-1}) observed here, suggesting that k_1 corresponds to the rate-limiting step of gc oxidation by H_2O_2 (at low [H_2O_2]), and that generation of the first intermediate species is a fast process following this step.

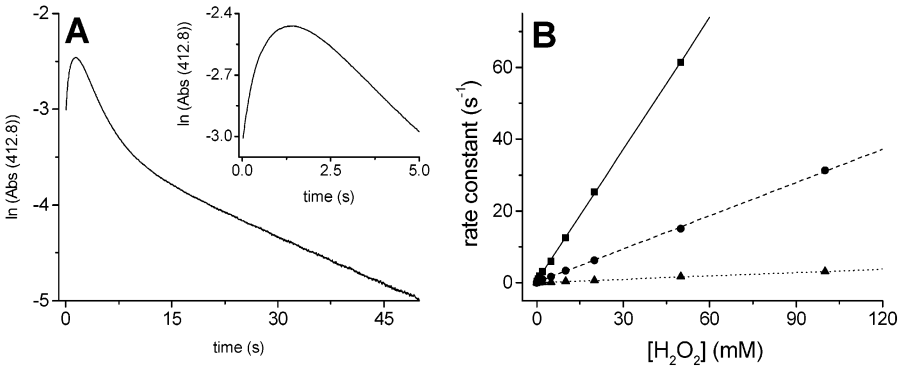

Figure 4. (a) Stopped-flow trace at 412.8 nm of the reaction between 1 μM u-cytc550 and 0.5 mM H_2O_2 in the absence of gc. Inset: enlargement of part a, showing details of the first two phases. Note that the natural logarithm of the absorbance is shown. (b) Dependence on H_2O_2 of each of the three rate constants observed at 412.8 nm. The lines are linear fits to the data.

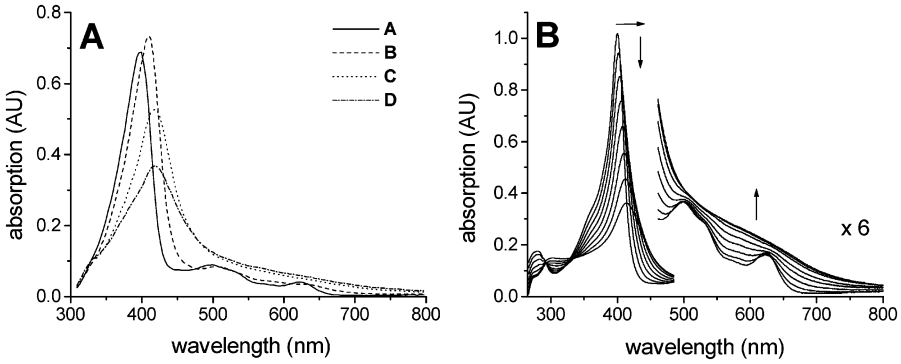

Figure 5. (a) Deconvoluted UV−vis spectra of the intermediates (as discussed in the text) observed in the reaction of u-cytc550 with H_2O_2 in the absence of gc. The spectra were simulated as discussed in the text. [H_2O_2] was 0.1 mM, and [u-cytc550] was 1 μM. (b) Spectral evolution of u-cytc550 following the successive addition of aliquots of 0.5 molar equiv of H_2O_2. The spectra were recorded each time after allowing the reaction to proceed to completion, and shown are respective spectra of u-cytc550 after addition of 0, 1, 2, etc., equiv of H_2O_2 peroxide (in the direction of the arrows).

The time dependence of the reaction between H_2O_2 and u-cytc550 was followed over the entire visible range, using a diode array. With the help of the previously determined rate constants, the time-dependent spectra were deconvoluted at various concentrations of H_2O_2 (using Scheme 1). The resulting simulated spectra of u-cytc550 (A) and intermediates B−D are shown in Figure 5a. The spectra of the final species (D) and the second intermediate (C) have a much less intense Soret band and are relatively featureless, while the first intermediate (B) has a slightly more intense, red-shifted Soret band and displays several distinct bands. The absorption maxima of each species are summarized in Table 1.

The effect of reductant on the spectral changes was examined by using sodium ascorbate. This was used instead of gc as a reductant because the oxidized product of the latter absorbs strongly in the region of interest (λ_{max} = 470 nm). In the presence of 20 mM sodium ascorbate, H_2O_2 causes a slow bleaching of the spectrum, with no evidence for intermediates. The final product, obtained after prolonged exposure to H_2O_2, shows a similar spectrum as the final spectrum obtained in the absence of sodium ascorbate, except that the broad absorption is now blue-shifted and has a distinct shoulder at 370 nm (not shown).

Next, it was assessed whether sodium ascorbate would react with the intermediate species in the reaction of H_2O_2 with u-cytc550. For this, u-cytc550 was reacted with a 50-fold excess of H_2O_2 for a set period, after which sodium ascorbate was added and the spectral evolution observed (final concentrations of reactants: 5 μM u-cytc550, 0.25 mM H_2O_2, and 10 mM sodium ascorbate). The incubation period with H_2O_2 was varied between 0 and 100 s, with the aim to maximize the expected concentrations of intermediates at the moment of addition of sodium ascorbate. For each incubation period, the addition of ascorbate had the sole effect of arresting spectral development (except for slow, continuous

Table 1. UV−vis Parameters of U-cytc550, of Intermediates in the Heme Degradation Pathway, and of Derivatives of the First Observable Degradation Intermediate[a]

Fe (III) Species				
Fe(III) u-cytc550	397	497	527 (sh)	623
intermediate B[b]	409	505	571 (sh)	635 (sh)
intermediate C[b]	418			
intermediate D[b]	417			
species **B**[c]	406	507	562 (sh)	633 (sh)
species **B**[c] + KCN	416	542		
Fe(III) hydroxyheme[d]	407	535 (sh)	575 (sh)	630 (sh)
Fe(II) Species				
Fe(II) u-cytc550	422	550		
species **B**[c] + dithionite	427	552	607 (sh)	
species **B**[c] + dithionite + EMS[e]	425	530	553	
Fe(II) hydroxyheme[f]	432	∼540[g]	635[g]	

[a] Conditions: 6 M Gdn·HCl, 100 mM sodium phosphate, pH 5.0. Peak maxima are in nm, and shoulders are indicated by "sh". [b] From simulated spectra of the intermediates observed transiently in the stopped-flow experiments. [c] "Species **B**" indicates the sample obtained by addition of 3 equiv of H_2O_2, as discussed in the text (and labeled **B** therein). [d] Ferric α-hydroxyheme in heme oxygenase at pH 7.0.[23] [e] Ethylmethyl sulfide. [f] Ferrous α-hydroxyheme in heme oxygenase at pH 7.0.[22] [g] Estimated from Figure 1 in Mansfield Matera et al.[22]

bleaching). Thus, no shift in the position of the Soret band was observed once ascorbate was added (not shown). Therefore, none of the observed reaction products of u-cytc550 with H_2O_2 are reverted by ascorbate, and thus, they are not part of the catalytic peroxidase cycle of u-cytc550.

The properties of the intermediates were also studied by controlled addition of H_2O_2. For this, H_2O_2 was added in aliquots of 0.5 molar equiv (with respect to u-cytc550), and the reaction was allowed to proceed to completion. Figure 5b shows the spectral evolution of u-cytc550 following this treatment. The spectral changes are very similar to those seen in the stopped-flow experiments. The spectrum obtained after the addition of ~3 equiv of H_2O_2 is similar to the spectrum obtained in the stopped-flow experiments after ~0.9 s (at 0.5 mM H_2O_2) and comparable to the simulated spectrum of the first intermediate (B). It can be calculated that the spectrum obtained after 0.9 s in the stopped-flow experiments contains ~60% of intermediate B and about 30% u-cytc550. Accordingly, the peak maxima of the spectrum of the sample obtained after addition of 3 equiv do not correspond exactly to the simulated spectrum of intermediate B (Table 1), but the general shapes of the spectra are very similar and it can be safely stated that the major species in the sample is **B**. The peroxidase activity of **B** thus obtained was measured, and it corresponds to ca. 35% of the activity of untreated u-cytc550 (not shown). This correlates well to the percentage of unmodified u-cytc550 expected and indicates that intermediate B has no or little peroxidase activity.

Properties of the First Observed Intermediate in the Peroxide-Driven Degradation of the Heme of U-cytc550. The sample obtained by the addition of 3 equiv of H_2O_2 to u-cytc550 was characterized further, as will be discussed next. The sample did not appear sensitive to O_2. When prepared under an argon atmosphere, it has the same optical spectrum as when prepared aerobically. The addition of 20 mM ascorbate or gc had no effect on the spectrum of the sample.

The addition of several equivalents of KCN caused significant shifts in the spectrum (Figure 6a, Table 1). With increasing pH, the peaks shift in the same direction as when KCN is added to the sample (Figure 6b), suggesting a transition from high spin to low spin ferric iron, due to binding of a strong ligand to the iron, possibly lysine[9] or hydroxide. The p$K_{a,app}$ of this transition is 6.9 ± 0.1 (Figure 6c), approximately half a unit higher than that for unmodified heme-iron of u-cytc550 under these conditions.[8,9]

When dithionite is introduced into the sample, its color changes from bronze to brilliant green. The resulting spectrum is shown in Figure 7a, and its peak maxima (Table 1) indicate high spin ferrous iron. The fact that dithionite can reduce **B**, but ascorbate cannot, indicates that the species has a low reduction potential. When ethylmethyl sulfide is added, the splitting of the α- and β-bands around 550 nm indicates formation of low spin ferrous iron (Figure 7a, Table 1). Ethylmethyl sulfide is a good ligand for ferrous iron in *c*-type hemes.[12]

(12) Schejter, A.; Plotkin, B. *Biochem. J.* **1988**, *255*, 353−356.

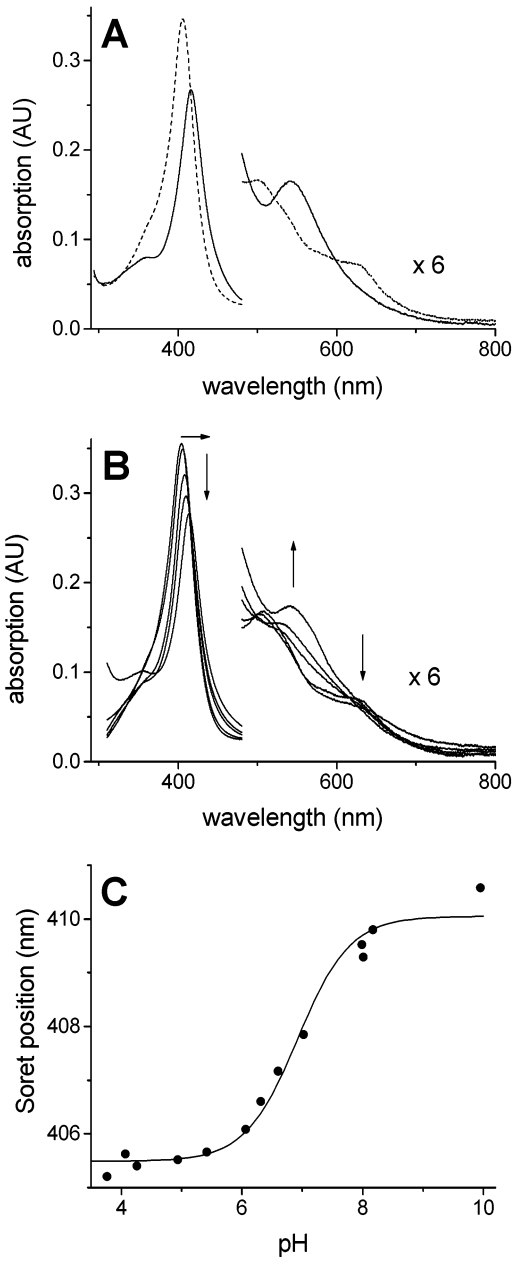

Figure 6. (a) UV−vis spectrum of u-cytc550 after addition of 3 equiv of H_2O_2 (- - -), and after the subsequent addition of 2 equiv of KCN (—). (b) Sample obtained after addition of 3 equiv of H_2O_2 at pH 5.0, adjusted to pH 1.04, 4.07, 7.02, 7.99, and 12.6, respectively. With increasing pH, the spectrum changes in the direction indicated by arrows. (c) pH dependence of the position of the Soret band of the sample obtained as in part b. The solid line (—) is the fit of the data to a single protonation event, yielding pK_a = 6.9 ± 0.1.

When subsequently the dithionite-reduced sample is exposed to oxygen, the brilliant green color is lost and the resultant spectrum is reminiscent of the original spectrum, except for a significantly bleached Soret band, and several other changes at lower wavelengths (Figure 7b). Additional cycles of dithionite addition followed by exposure to oxygen led to a species with a severely bleached and broad Soret band at ~387 nm and relatively intense and sharp peaks at 533 and 652 nm. This is shown in Figure 7c, together with a sample of verdoheme-cytc550 under the same conditions. The clear similarity between both spectra indicates that

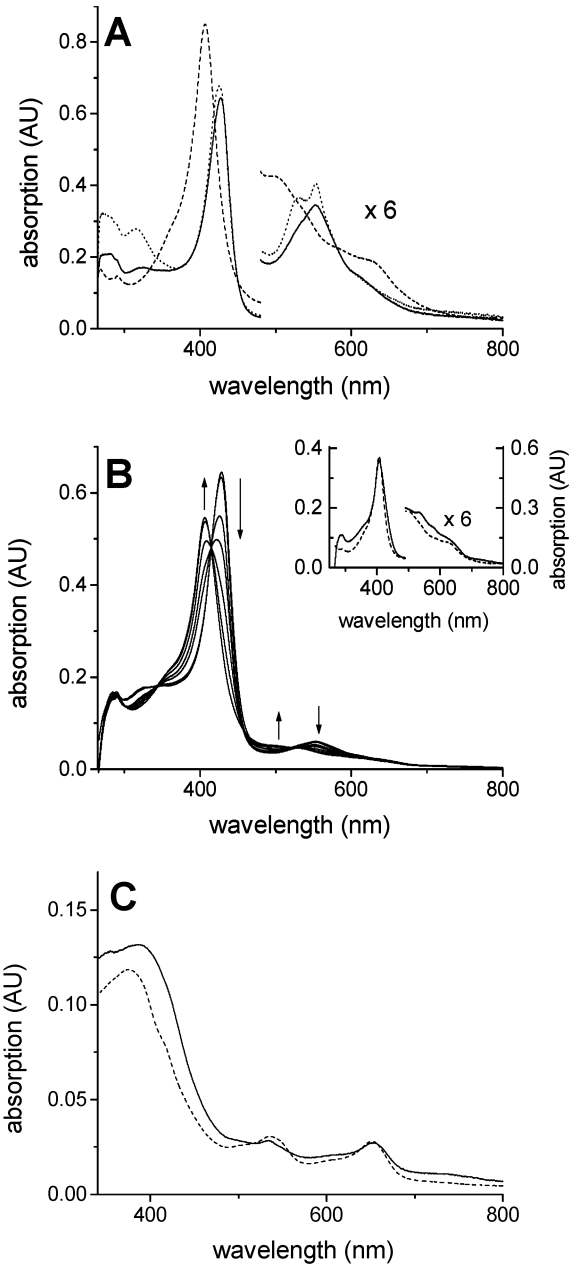

Figure 7. (a) UV−vis spectrum of u-cytc550 after addition of 3 equiv of H_2O_2 (- - -), after subsequent addition of sodium dithionite (—), and after addition of ethylmethyl sulfide in the presence of sodium dithionite (- - -). (b) Spectral evolution of the sample obtained after addition of 3 equiv of H_2O_2 and subsequently exposed to several cycles of addition of sodium dithionite followed by O_2. The arrows indicate the direction of the spectral changes following this treatment. Inset: the sample untreated and treated with a single cycle of dithionite/O_2, respectively. The left and right vertical scales are for untreated and treated samples, respectively. (c) Spectrum (- - -) of verdoheme-cytc550 in 6 M Gdn·HCl. This was prepared by a procedure similar to that described,[18] i.e., by prolonged exposure of u-cytc550 to 20 mM sodium ascorbate and a stream of O_2. The solid line (—) is the spectrum of the sample obtained after addition of 3 equiv of H_2O_2 and >10 cycles of successive exposure to sodium dithionite and O_2.

verdoheme-cytc550 is formed when **B** is exposed to oxygen in the presence of dithionite.

The EPR spectrum of the sample obtained by addition of 3 equiv of H_2O_2 is shown in Figure 8, together with a spectrum of unmodified u-cytc550. The major signal in the spectrum of unmodified u-cytc550 is from high spin ferric

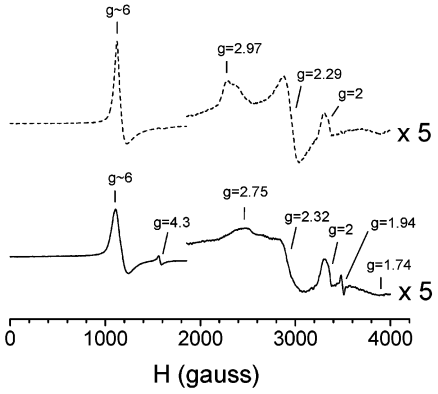

Figure 8. X-band EPR spectra of u-cytc550 (- - -) and u-cytc550 after addition of 3 equiv of H_2O_2 (—). The samples contained approximately 1 mM protein and were in 30% glycerol, 4.2 M Gdn·HCl, 70 mM sodium phosphate. The sample of u-cytc550 and that after addition of 3 equiv of H_2O_2 were at pH 5.3 and 5.4, respectively. The positive signal at $g = 2.04$ is an artifact of the resonator.

heme with typical g-values at $g = 6$ and $g = 2$. A minor signal is present which belongs to low spin ferric heme, with g-values at 2.97 and 2.29. U-cytc550 experiences a pH-dependent spin state change, with $pK_{a,app} = 6.33$,[9] and thus, at the pH of the sample (pH= 5.3), about 10% of u-cytc550 is expected to be low spin. The EPR spectrum of the peroxide-modified u-cytc550 also shows multiple signals (Figure 8). The major signal belongs to high spin ferric heme, but the signal at $g = 6$ is somewhat broadened with respect to the $g = 6$ signal of unmodified u-cytc550. In addition, the low spin heme signal has also changed ($g = 2.75$, 2.32, and 1.74). At the pH of the experiment (pH = 5.4), about 3% of **B** is expected to be low spin ($pK_{a,app} = 6.9$, vide supra), and thus, the low spin and high spin signals are both ascribed to **B**. The significant change in the low spin heme signal, along with the broadened high spin signal at $g = 6$, corroborates that the peroxide-driven modifications are in the immediate vicinity of the heme-iron, i.e., either on the heme macrocycle or on the axial His ligand. The spectrum of the peroxide-modified u-cytc550 also exhibits signals at $g = 4.3$ and $g = 1.94$. Both signals are also present in the sample containing unmodified u-cytc550, albeit much less intense, and both have increased by an equal amount in the modified u-cytc550 sample. The signal at $g = 4.3$ is assigned to non-heme high spin iron, while the signal at $g = 1.94$ currently remains unassigned.

Discussion

In the presence of H_2O_2, u-cytc550 is converted into a peroxidase-inactive form. This is obvious from the product formation curve (Figure 1) and is observable by changes in the optical properties of u-cytc550 (Figure 4). The dependence of the inactivation rate constant on [H_2O_2] is hyperbolic (Figure 2a), which suggests the presence of an intermediate species (termed labile intermediate here) in the H_2O_2-mediated inactivation process. In the presence of reducing substrate, gc, the inactivation is slowed. The protective effect of gc also displays a hyperbolic dependence, but at saturating gc, the inactivation still takes place with an appreciable rate (Figure 2b). When gc exerts its protective effect by lowering

Table 2. Kinetic Parameters for the H_2O_2-Driven Inactivation of U-cytc550 and for the Catalytic Conversion of gc[a]

kinetic parameters for inactivation[b]		kinetic parameters for catalysis[c]	
k_A	7.3 mM s^{-1}	k_{cat}	707 ± 26 s^{-1}
k_B	1.64 s^{-1}		
K_{inact}^{gc}	10.8 mM	K_M^{gc}	4.7 ± 0.3 mM
$K_{inact}^{H_2O_2}$	232 mM	$K_M^{H_2O_2}$	236 ± 14 mM

[a] Conditions: 298 K, 100 mM Na−phosphate pH 5.0, 6 M Gdn·HCl. [b] Values of the inactivation parameters obtained by fitting the data in Figure 2a,b to eq 2, assuming that $K_0 \rightarrow 0$. [c] From ref 8.

the steady-state concentration of the labile intermediate, models describing the hyperbolic H_2O_2-dependence of inactivation and hyperbolic form of the substrate protection take the general form of eq 2 (see Supporting Information for a derivation):

$$\text{inactivation rate constant} = \frac{(k_A + k_B[gc])[H_2O_2]}{K_0 + K_{inact}^{gc}[H_2O_2] + K_{inact}^{H_2O_2}[gc] + [H_2O_2][gc]} \quad (2)$$

The kinetics of inactivation were fitted to this function (solid lines in Figure 2a,b), yielding values for the catalytic constants as summed in Table 2. Herein the catalytic constants k_A and k_B, respectively, denote the gc-independent and gc-dependent inactivation rate constants, and K_{inact}^{gc} and $K_{inact}^{H_2O_2}$ are the apparent overall dissociation constants of u-cytc550 with gc and H_2O_2, respectively. K_0 was neglected in the fitting procedure as it can be shown to be small.

Previously,[8] we determined the kinetics of the H_2O_2-driven conversion of gc by u-cytc550. It was concluded that this proceeded through a ping-pong-type mechanism. First, HO_2^- binds to the heme-iron, and this peroxo-iron complex presumably then converted to an oxidizing intermediate capable of gc oxidation (Figure 9). The kinetics of substrate conversion are described by eq 3:

$$\text{turnover rate constant} = \frac{k_{cat}[gc][H_2O_2]}{K_M^{gc}[H_2O_2] + K_M^{H_2O_2}[gc] + [H_2O_2][gc]} \quad (3)$$

Combining this information with the above-mentioned inactivation characteristics makes it attractive to envisage that inactivation and catalytic turnover have at least one intermediate in common. Not only is H_2O_2 the essential reactant in both processes, but also gc is competent to participate in either process. The similarity in the values of K_{inact}^{gc} and $K_{inact}^{H_2O_2}$ with K_M^{gc} and $K_M^{H_2O_2}$, respectively, supports this (Table 2). Two likely candidates for the labile intermediate are the iron-peroxo species and the oxidizing intermediate (either or not in complex with the reducing substrate, gc), respectively, as is shown in Figure 9. Note that the former case requires that the conversion from iron-peroxo heme to the oxidizing intermediate is a reversible reaction.

The catalytic efficiency (CE), i.e. the number of turnovers per molecule of u-cytc550 before full inactivation of u-cytc550, is nearly independent of $[H_2O_2]$, but it shows a clear

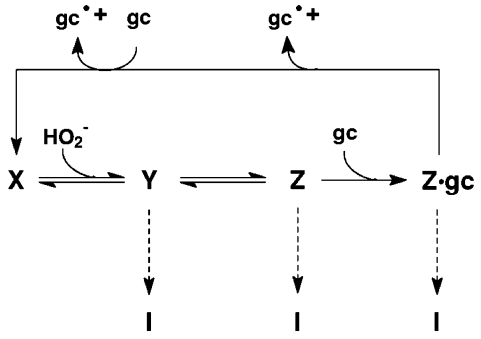

Figure 9. Purported peroxidase mechanism of u-cytc550, including possible inactivation pathways, based on this and previous work,[7,8] and by analogy to the mechanism of microperoxidase.[30] Both u-cytc550 and microperoxidase share the same catalytic center and have comparable activities.[8−10,30] Resting state, ferric protein is indicated by X, and the first intermediate, peroxo-iron is indicated by Y. Z represents the second intermediate, which in the text is referred to as the oxidizing intermediate. This is probably a ferryl species plus a radical cation.[30] The labile intermediate that leads to inactivated u-cytc550 (indicated by I) is either species Y, Z, or Z·gc. In the case that Y is the labile form leading to I, the conversion of Y to Z is reversible.

hyperbolic dependence on [gc] (Figure 3). The CE is the ratio between the rate constants of formation of oxidized gc (product) and of catalyst inactivation (see ref 13 and Supporting Information) and can consequently be described by eq 4a. With K_0 small, and considering the similarity of K_M and K_{inact} for both gc and H_2O_2 (Table 2), eq 4a can be approximated by eq 4b.

$$CE = \frac{k_{cat}[gc][H_2O_2]}{K_M^{gc}[H_2O_2] + K_M^{H_2O_2}[gc] + [H_2O_2][gc]} \cdot \frac{K_0 + K_{inact}^{gc}[H_2O_2] + K_{inact}^{H_2O_2}[gc] + [H_2O_2][gc]}{(k_A + k_B[gc])[H_2O_2]} \quad (4a)$$

$$\approx \frac{k_{cat}[gc]}{k_A + k_B[gc]} \quad (4b)$$

Equation 4b predicts that the CE is independent of $[H_2O_2]$ but should show a hyperbolic dependence on [gc]. The gc concentration at which the CE is half-maximal corresponds to k_A/k_B (4.5 mM, from Table 2), in fair agreement with the observed value (3.7 ± 0.3 mM). From eq 4, the CE at saturating gc equates to k_{cat}/k_B. Its calculated value is 431 (using a value of 707 s^{-1} for k_{cat} from previous work[8]), which is also in reasonable agreement with observation (534 ± 10).

In the absence of gc, H_2O_2 drives the formation of an optically distinct form of u-cytc550 (Figures 4 and 5). The rate of this reaction is linearly dependent on $[H_2O_2]$ at the concentrations studied, with a bimolecular rate constant k_1 (Scheme 1) of 1226 M^{-1} s^{-1}. This is close to the bimolecular rate constant of the reaction with H_2O_2 for substrate conversion during catalysis (1500 M^{-1} s^{-1}).[8] Thus, at low $[H_2O_2]$, the rate-limiting step is the same for both catalysis and peroxide-driven heme modification. Again, this places a clear link between the two processes. The properties of

(13) Fersht, A. R. *Enzyme Structure and Mechanism*, 2nd ed.; W. H. Freeman and Company: New York, 1985; p 118.

the peroxide-modified forms of u-cytc550 may thus help understand the peroxide-driven inactivation of u-cytc550.

U-cytc550 is modified by H_2O_2 in three separate, consecutive steps (Figures 4 and 5). The kinetics of the first step render this the most relevant with respect to the inactivation mechanism. The optical properties of the first intermediate in the peroxide-driven heme modification pathway are very similar to those obtained after addition of 3 equiv of H_2O_2 to u-cytc550 (Figure 5). This indicates that the major species in the sample obtained by addition of 3 equiv of H_2O_2 is the first observable intermediate (**B**) and allows for use of this sample to investigate its properties.

The optical spectrum of **B** indicates modification of the heme periphery or of the axial His ligand. Compared to unmodified u-cytc550, the absorption bands have become less well defined and are significantly red-shifted (Figure 5, Table 1). The iron is high spin, i.e., with a weak or absent sixth ligand, and can go low spin by the addition of KCN, and by an increase in the pH (Figure 8). **B** cannot be reduced by ascorbate, but in the presence of dithionite, a typical high spin ferrous heme spectrum results. As with the ferric protein, the absorption bands are red-shifted in ferrous **B** with respect to unmodified ferrous u-cytc550 (Table 1). Addition of ethylmethyl sulfide, a strong ligand for ferrous heme-*c*,[12] results in a typical low spin ferrous heme spectrum (Figure 7). The red shift of absorption bands in both ferrous and ferric **B** with respect to u-cytc550 suggests that the peroxide-driven modification involves an electron-withdrawing substituent on the porphyrin ring, or a less electronegative iron center.[14] This is corroborated by the elevated $pK_{a,app}$ of the high to low spin transition of ferric **B** compared to unmodified u-cytc550 ($pK_{a,app} = 6.9$ and 6.33, respectively).

When dithionite-reduced **B** is exposed to O_2, immediate changes take place in the optical spectrum that suggest reoxidation of **B**, along with additional modifications (Figure 7). Several cycles of exposure to dithionite and O_2 yield a species with a spectrum closely resembling that of verdoheme-cytc550 (Figure 7). Thus, it is assumed that **B** is a precursor to verdoheme. There are two well-described pathways leading to verdoheme generation, i.e., the heme oxygenase pathway and coupled oxidation.[15−18] In both of these pathways, the first heme modification step is hydroxylation of the porphyrin at one of the meso positions, usually the α-meso position.[15,16] α-Hydroxyheme is easily generated by the addition of H_2O_2 to the ferric heme-containing heme oxygenase,[19−21] indicating that **B** may also contain this heme-derivative.

The likelihood that **B** is hydroxyheme-cytc550 is substantiated by the similarity in the optical spectra of ferrous and especially ferric **B** to that of ferrous and ferric α-hydroxyheme (Table 1). In the EPR spectrum, the slightly broadened (with respect to u-cytc550) high spin heme signal at $g = 6$ (Figure 8) is in keeping with that reported for α-hydroxyheme-bound heme oxygenase.[21,22] It is interesting, however, that, unlike for α-hydroxyheme-containing heme oxygenase and myoglobin,[21−23] no radical signal at $g = 2$ is observed in the EPR spectrum of **B**. The radical signal originates from one of the resonance structures of α-hydroxyheme, due to charge-transfer resulting in a porphyrin-based radical and ferrous iron.[15,16,21−25] The strong reactivity of α-hydroxyheme with O_2 commonly is associated with this resonance structure, which requires deprotonation of the meso-hydroxyl.[15,16,22,23,26] On the other hand, ferric **B** is not reactive with O_2, which agrees with the absence of radical character in this species. The apparent lack of a ferrous-radical resonance form in hydroxyheme-cytc550 may be related to the specific structure of the *c*-type heme of cytc550, i.e., the covalent link to the protein matrix through thioether bonds between two cysteines and the vinyl substituents. Possibly associated to this is the observation that porphyrins with electron-withdrawing groups in place of the vinyls are converted only slowly by heme oxygenase.[27]

As discussed, the peroxidase inactivation kinetics of u-cytc550 indicate the presence of a labile intermediate on the catalytic pathway. Two possible candidates emerge from the inactivation kinetics, namely the peroxo-iron species or the oxidizing intermediate (probably a ferryl species such as compound I in peroxidases). The identification of hydroxyheme-cytc550 as the first observable intermediate in the peroxide-driven heme modification pathway provides support for the peroxo-iron species as the labile intermediate as this species is the direct precursor of α-hydroxyheme in heme oxygenase.[15,16,28] As proposed by Ortiz de Montellano for heme proteins in general, the peroxo-iron species can either react further to the ferryl species or it can hydroxylate the porphyrin ring in an intramolecular oxygen-transfer reaction.[16,29]

If this were the case for u-cytc550 as well, it implies that the conversion from peroxo-iron intermediate to the oxidizing

(14) Moore, G. R.; Pettigrew, G. W. *Cytochromes* c. *Evolutionary, Structural and Physicochemical Aspects*; Springer-Verlag: Berlin-Heidelberg, Germany, 1990.
(15) Yoshida, T.; Taiko Migita, C. *J. Inorg. Biochem.* **2002**, *82*, 33−41.
(16) Ortiz de Montellano, P. R.; Wilks, A. *Adv. Inorg. Chem* **2001**, *51*, 359−407.
(17) Balch, A. L.; Latos-Grażyński, L.; Noll, B. C.; Olmstead, M. M.; Szterenberg, L.; Safari, N. *J. Am. Chem. Soc.* **1993**, *115*, 1422−1429.
(18) Lagarias, J. C. *Biochemistry* **1982**, *21*, 5962−5967.
(19) Wilks, A.; Ortiz de Montellano, P. R. *J. Biol. Chem.* **1993**, *268*, 22357−22362.
(20) Ishikawa, K.; Takeuchi, N.; Takahashi, S.; Mansfield Matera, K.; Sato, M.; Shibahara, S.; Rousseau, D. L.; Ikeda-Saito, M.; Yoshida, T. *J. Biol. Chem.* **1995**, *270*, 6345−6350.
(21) Liu, Y.; Moënne-Loccoz, P.; Loehr, T. M.; Ortiz de Montellano, P. R. *J. Biol. Chem.* **1997**, *272*, 6909−6917.
(22) Mansfield Matera, K.; Takahashi, S.; Fujii, H.; Zhou, H.; Ishikawa, K.; Yoshimura, T.; Rousseau, D. L.; Yoshida, T.; Ikeda-Saito, M. *J. Biol. Chem.* **1996**, *271*, 6618−6624.
(23) Sakamoto, H.; Omata, Y.; Palmer, G.; Noguchi, M. *J. Biol. Chem.* **1999**, *274*, 18196−18200.
(24) Morishima, I.; Fujii, H.; Shiro, Y.; Sano, S. *Inorg. Chem.* **1993**, *34* (4) 1528−1535.
(25) Morishima, I.; Fujii, H.; Shiro, Y. *J. Am. Chem. Soc.* **1986**, *108*, 3858−3860.
(26) Balch, A. L.; Latos-Grażyński, L.; Noll, B. C.; Olmstead, M. M.; Zovinka, E. P. *Inorg. Chem.* **1992**, *31*, 2249−2255.
(27) Frydman, R. B.; Tomaro, M. L.; Buldain, G.; Awruch, J.; Díaz, L.; Frydman, B. *Biochemistry* **1981**, *20*, 5177−5182.
(28) Davydov, R.; Kofman, V.; Fujii, H.; Yoshida, T.; Ikeda-Saito, M.; Hoffman, B. M. *J. Am. Chem. Soc.* **2002**, *124*, 1798−1808.
(29) Liu, Y.; Lightning, L. K.; Huang, H.-W.; Moënne-Loccoz, P.; Schuller, D. J.; Poulos, T. L.; Ortiz de Montellano, P. R. *J. Biol. Chem.* **2000**, *275*, 34501−34507.

intermediate is reversible, with a substantial rate for the back reaction. Although this by no means is the current consensus for peroxidases, evidence in favor of reversibility is accumulating for microperoxidases (see Veeger's work[30] and references therein), which are highly comparable to u-cytc550.[8,9]

The work described here demonstrates that the peroxide-driven inactivation of u-cytc550 is caused by an intrinsic tendency for autodestruction of one of the intermediates in the catalytic peroxidase cycle. This intermediate is probably the peroxo-iron species, but a role for an alternative species cannot be excluded. Minimization of the steady-state concentration of this labile intermediate is likely to enhance the catalytic efficiency of u-cytc550, pointing out a possible way to improve its applicability as a catalyst.

Interestingly, for horseradish peroxidase (HRP), the catalytic efficiency is much decreased upon replacement of the distal Arg and His residues.[31−33] These residues are essential for formation of the oxidizing intermediate (compound I) in HRP, both accelerating binding of H_2O_2 and generation of compound I from the (hydro)-peroxo-iron complex.[31,34] The distal Arg is thought to play an important role in the latter reaction by stabilizing the transition state for the heterolytic cleavage of the peroxide O−O bond.[31,34−36] In an HRP mutant whereby the Arg was replaced by Leu, the rate of the latter reaction was sufficiently decreased to allow direct observation of a peroxo-iron species.[36] Moreover, compound I in this mutant was much less reactive toward reducing substrates. The fact that this mutant displays a much poorer CE supports our conclusions, despite differences in the H_2O_2-driven inactivation mechanism of HRP and u-cytc550.[31,32]

Acknowledgment. This work was supported by the Foundation for Chemical Research (SON) and the Foundation for Technical Sciences (STW) with financial aid from the Netherlands Organisation for Scientific Research (NWO), and performed under the auspices of the BIOMAC Graduate Research School of Leiden and Delft.

Supporting Information Available: Derivation of eq 2. This material is available free of charge via the Internet at http://pubs.acs.org.

IC0343861

(30) Veeger, C. *J. Inorg. Biochem.* **2002**, *91*, 35−45.
(31) Veitch, N. C.; Smith, A. T. *Adv. Inorg. Chem.* **2001**, *51*, 107−162.
(32) Arnao, M. B.; Acosta, M.; del Río, J. A.; Varón, R.; García-Cánovas, F. *Biochim. Biophys. Acta* **1990**, *1041*, 43−47.
(33) Hiner, A. N. P.; Hernández-Ruíz, J.; García-Cánovas, F.; Smith, A. T.; Arnao, M. B.; Acosta, M. *Eur. J. Biochem.* **1995**, *234*, 506−512.
(34) Hiner, A. N. P.; Raven, E. L.; Thorneley, R. N. F.; García-Cánovas, F.; Rodríguez-López, J. N. *J. Inorg. Biochem.* **2002**, *91*, 27−34.
(35) Rodríguez-López, J. N.; Smith, A. T.; Thorneley, R. N. F. *J. Biol. Inorg. Chem.* **1996**, *1*, 136−142.
(36) Rodríguez-López, J. N.; Smith, A. T.; Thorneley, R. N. F. *J. Biol. Chem.* **1996**, *271*, 4023−4030.